NIR spectroscopic survey of obscured AGNs at z~2

Masayuki Akiyama (Astronomical Institute, Tohoku Univ.), Tomohiro Yoshikawa (Kyoto Sangyo Univ.), Dave Alexander (Durham Univ.)

In order to reveal statistical properties of obscured AGNs in the peak epoch of QSO activities, i.e. z~2, we are conducting NIR spectroscopic surveys of optically-faint Xray sources using unique NIR MOS instruments of Subaru, Multi-Object Infrared Camera and Spectrograph (MOIRCS) and Fiber Multi-Object Spectrograph (FMOS). NIR spectroscopic suverys revealed a large number of obscured AGNs among optically-faint X-ray sources in the redshift range as expected from photometric redshift estimations. In order to unveil further obscured populations of AGNs which cannot be detected even in hard X-ray surveys, we are proposing a NIR spectroscopic survey of photometrically-selected massive galaxies at z~2.

Large Number of Obscured AGNs at z=1-3 ?

In order to reveal the accretion growth history of Super Massive Black Holes (SMBHs), X-ray surveys with various depth and area have been conducted so far. Multi-wavelength follow-up observations revealed their physical nature, i.e. redshifts, luminosities, etc. In Figure 1, the redshifts and i-band magnitudes of X-ray sources found in the Subaru XMM-Newton Deep Survey (SXDS) field is shown. In the left panel, AGNs identified by optical spectroscopic observation are shown. Optical spectroscopic observations successfully identified AGNs brighter than i~23.5mag. In the left panel, AGNs without spectroscopic identifications are plotted with redshifts estimated with photometry in 15 broad-bands from FUV to MIR. The photometric redshift estimation suggests that there are large number of obscured AGNs exist among opticall-faint X-ray sources in the redshift range between 1-3. Redshift distribution of total (thin) and specz (thin) samples are shown in Figure 2. The redshift distributions imply obscured narrow-line AGN population significantly contribute AGN number density in the redshift range.

Figure 1

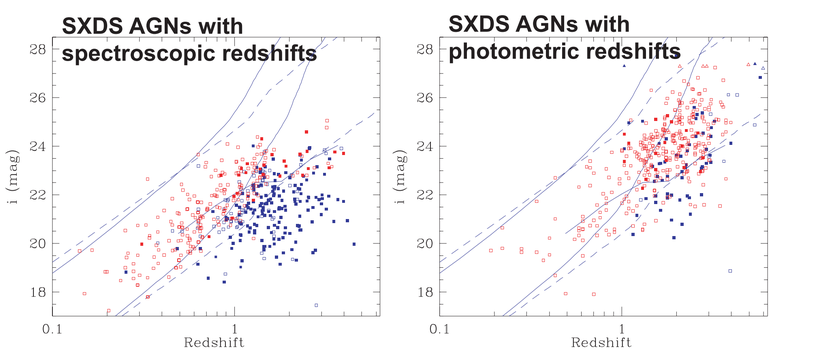

Figure 2

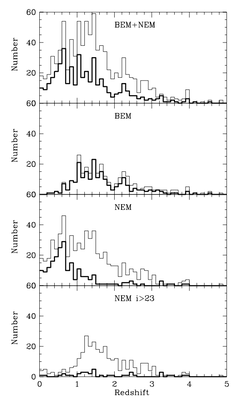

Summary of NIR spectroscopic survey observations

Optically-faint X-ray sources always have red optical-NIR color, thus part of the optically-faint X-ray sources are within reach of NIR spectroscopic observations with 8-10m class telescopes. Additionally, strong rest-frame optical emission lines fall in the NIR wavelength for objects at z>1. In order to reveal the nature of optically-faint X-ray sources, we conducted NIR spectroscopic survey observations of optically-faint X-ray sources with Subaru/MOIRCS. MOIRCS is a multi-slit NIR spectrograph with fov of 4' x 7'. We used R=500 low-resolution grism with z+J+H or H+K bands coverage. We observed 2 fovs in SXDS with 1.5h-3.8h in Nov.2006, and 4 fovs in CDFN with 2.7h-5.3h (HK500) in Mar.2007 (as shown in the left panel of Figure 3). Sample spectrum of a type-2 AGN at z=1.57 is shown in the upper panels of Figure 3. Strong Ha and [OIII] lines are detected and large [NII]/Halpha and [OIII]/Hbeta line ratios are consistent with local Seyfert 2 AGNs. On the contrary, part of the object only show strong narrow Ha emission line like two objects shown in the bottom of Figure 3. From about half of the objects, we detected emission lines.

Summary of the NIR spectroscopic identification is shown in Figure 4 in the K vs. V-K diagram. AGNs are separated at z=1.5 based on z_spec or z_phot. Red symbols indicate objects observed in the NIR. Filled red circles show objects identified with NIR emission line, open red circles show observed objects of which continuum was detected but no emission line, and red crosses show objects without continuum and emission line. With a few hours integration, continuum was detected from objects brighter than KAB<22.5, and about half of them are identified with emission lines. In Figure 5, spectroscopic redshifts obtained with the NIR observations vs. photometric redshift is shown. The estimated photometric redshifts are roughly consistent with the spectroscopic redshifts. Unidentified objects are plotted vertically at around z~1(KAB<22.5) and z~0.5(KAB>22.5). There is no clear difference of photometric redshift distributions of identified and un-identified AGNs except for that fainter objects have larger z_phot.

Figure 3

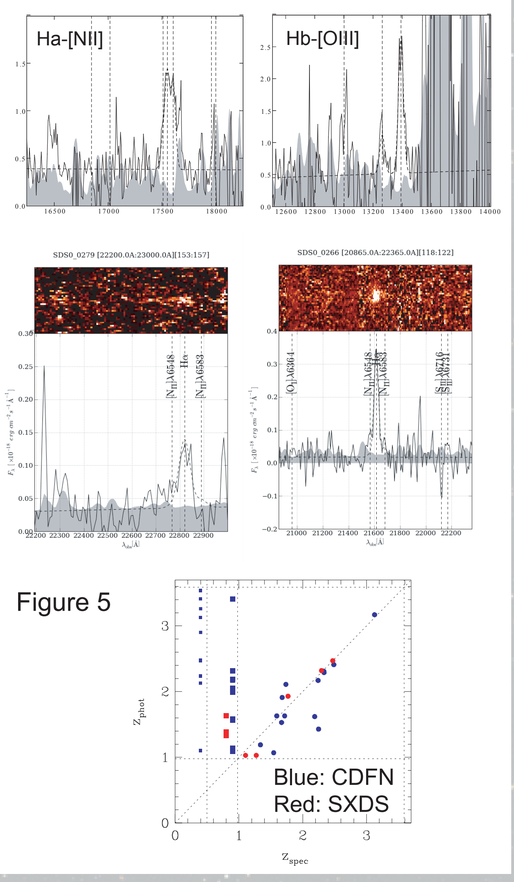

Figure 4

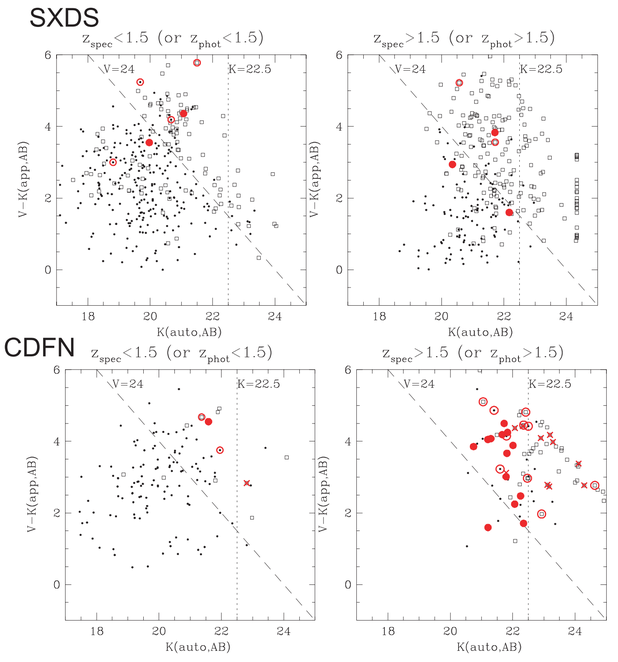

Figure 5

Properties of NIR identified / non-identified AGNs

NIR identified and un-indentified AGNs are plotted on the redshift vs. i-band magnitude diagram in Figure 6 (left SXDS, right CDFN samples). All of them follows the redshift-magnitude sequence of narrow-line AGNs. Rest-frame optical light of narrow-line AGNs is thought to be dominated by host galaxy emission, because their SED is described well with SED templates of galaxies. The tight redshift-magnitude sequence of narrow-line AGNs suggests that the stellar masses of the host galaxies are roughly constant. i-band magnitude track of galaxy models are shown with solid and dashed lines. Most of the narrow-line AGNs are distributed within the region enclosed by the dashed lines and the NIR identified and un-identified AGNs roughly follows the sequence. There is no clear difference in the diagram between the NIR identified and un-identified AGNs.

Luminosities of X-ray selected AGNs are plotted as a function of redshift in Figure 7. NIR identified and un-identified AGNs are plotted with red symbols. Because of the difference of the flux limits, the typical luminosity of the samples is different between SXDS and CDFN. Even though the large difference in the typical luminosity, there is no clear difference of the NIR identification rates of SXDS and CDFN. Additionally, there is no clear dependence of luminosity distribution of NIR identified and un-identified AGNs in each sample.

In Figure 8, the hardness ratio distribution of the X-ray sources are shown as a function of redshifts. Again, there is no difference between the identified and un-identified AGNs in the diagram.

Considering that there is no clear difference between the NIR identified and un-identified AGNs, the difference of emission line detection may be caused by the scatter of the ratio between hard X-ray flux and H-alpha flux. Because NIR observations can be affected by strong night sky emission lines, the sensitivity strongly depends on the wavelength. Therefore, the dependence of line sensitivity on wavelength may affect the non-detection of un-identified AGNs. However, it should be noted that more than 80% of the covered wavelength range is roughly uniformly covered even in the low-resolution observation, therefore the wavelength dependence only cannot explain the emission line detection rate.

Figure 6

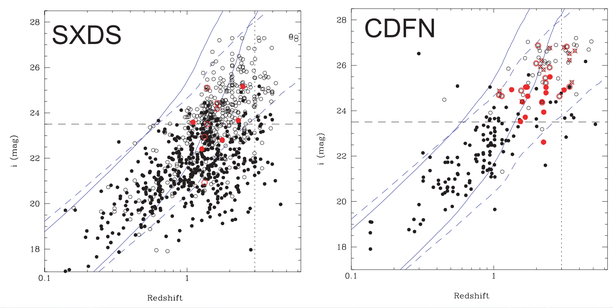

Figure 7

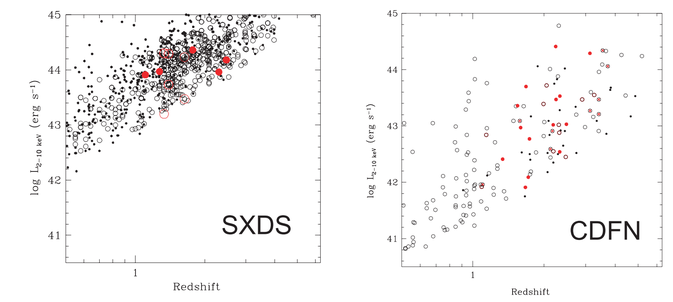

Figure 8

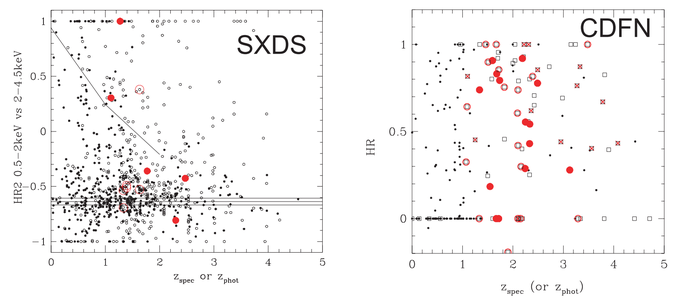

Future wide-field X-ray AGN and Compton-thick AGN surveys with FMOS

As shown above, NIR spectroscopic survey is successful in identifying obscured hard X-ray AGNs at z=1-3. Currently another NIR multi-object spectrograph, Fiber Multi-Object Spectrograph (FMOS) is under commissioning on Subaru telescope. The spectrograph can observe 400 objects in 30' fov simultaneously in z-H band. Large number of optically-faint X-ray sources in wide field survey regions (SXDS etc.) are still unidentified, but such sources can be observed with FMOS.

Additionally, in order to search heavily obscured AGNs which cannot be detected in deep X-ray surveys, we are proposing NIR spectroscopic survey observation for massive galaxies at z=1.3-1.6.The galaxies are selected based on photometric redshifts. Considering most of the X-ray selected AGNs are reside in galaxies with stellar mass logMstar>10.5, we will select target galaxies with photometric redshifts and stellar masses. With low-resolution mode of FMOS, we can cover H-alpha+[NII] and H-beta+[OIII] emission line regions simultaneously. 2.5 hours integration with FMOS, we can detect F[OIII]=2.0x10^-16 erg s-1 cm-2 emission line with SN=10. Acieving this sensitivity, we can detect AGNs with obscuration corrected hard X-ray luminosity of 1.4x10^44 erg s-1. Based on the number density estimate of the Compton-thick AGNs in the redshift range (see Figure 9), we expect more than 50 heavily-obscured AGNs can be detected with the blind emission line search among massive galaxies in SXDS.

Figure 9

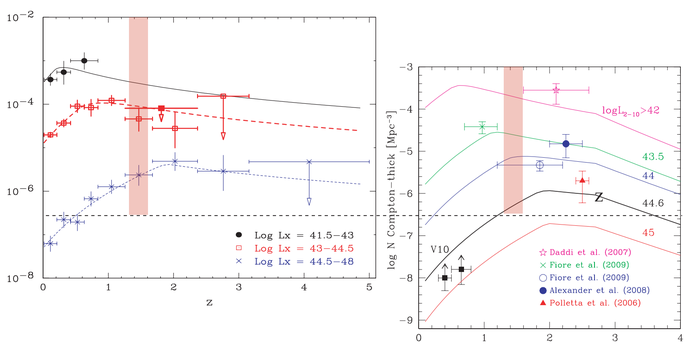

Left) Number density of X-ray selected AGNs from Ueda et al. (2003). Almost all of these AGNs are non-Compton-thick AGNs. Right) Estimated number density of Compton-thick AGNs in each luminosity bin as a function of redshift (Vignali et al. 2010). The proposed spectroscopic survey prove the redshift and number density (=volume) range hatched with orange.